Comparison of NOAA/NASA PAL and NOAA GVI Data for Vegetation Change Studies over China

Stephen S. Young and Assaf Anyamba

Abstract

Remotely sensed data, especially that from the Advanced Very High Resolution Radiometer (AVHRR), are increasingly being used to analyze changes in the global environment. This research analyzes two of the most commonly used remote sensing data sets for global environmental change research, the National Oceanic and Atmospheric Administration's (NOAA) Global Vegetation Index (GVI) data and the new NOAA/National Aeronautics and Space Administration's (NASA) Pathfinder AVHRR Land (PAL) data set, to determine if the new PAL data have successfully removed the major sensor-related problems found in the GVI data. Principal Components Analysis of the data for the geographic region of China is used with results indicating that sensor-related problems remain in the PAL data, though not as severely as in the GVI data. For the time period of 1982 to 1992, the GVI and PAL data suffer from problems of spatial misregistration and radiometric miscalibration. The problem of orbital drift, however, has been minimized in the PAL data.

Introduction

Global environmental change research is rapidly rising in importance (NAS, 1990; IGBP, 1994) with an increasing need for a large amount of geographically referenced data (Townshend, 1992). Remotely sensed data is an important source for deriving global data because of its internal consistency, its reproducibility, and its ability to cover areas where land-cover data are sparse (DeFries *et al.*, 1995). In the 1980s and early 90s, Landsat and SPOT provided high spatial resolution images of the Earth's surface for regional land-cover applications. In order to monitor vegetation at the global scale, however, the research community has increasingly turned to data from meteorological satellites, and, in particular, to the National Oceanic and Atmospheric Administration (NOAA) series with the Advanced Very High Resolution Radiometer (AVHRR) sensor (Ehrlich *et al.*, 1994). The AVHRR sensor, with its wide instantaneous field-of-view produces a spatial resolution of approximately 1.1 km by 1.1 km at nadir, and has the ability to sense the entire Earth every day. The scanner records electromagnetic energy data in five channels: channel 1, red (0.58 to 0.68 μm); channel 2, near infrared (NIR) (0.725 to 1.1 μm); channel 3, middle infrared (3.55 to 3.93 μm); and two thermal bands, channel 4 (10.5 to 11.5 μm) and channel 5 (11.5 to 12.5 μm). To overcome the problems of large data sets and high data costs, NOAA produces a daily Global Area Coverage (GAC) data set. GAC data are formed by resampling 1.1-km AVHRR data on-board the NOAA satellites to a resolution of approximately 4.4 km at nadir, at the equator. GAC data are further re-sampled by NOAA and other users to spatial resolutions of 8, 16, and 32 km. A widely used derivative of the GAC data is a Global Vegetation Index (GVI) which is a 16-km resolution Normalized Difference Vegetation Index (NDVI)[1]. Early GVI studies were applied at the regional scale (Tucker *et al.*, 1984; Malingreau *et al.*, 1985), followed by larger continental- and global-scale studies (Box *et al.*, 1989; Tateishi and Kajiwara, 1992).

Although it was originally designed to monitor meteorological phenomena, the measurements in the red and NIR spectral bands make the data very useful for vegetation analysis. In part because of the wide availability of the data, researchers have found a multitude of applications in vegetation research, meteorology, oceanography, and geology (Thomas *et al.*, 1989; Ehrlich *et al.*, 1994). Satellite-based remote sensing employs the same measurement device over the entire globe, making it particularly suitable for global studies compared with ground-based surveys. However, the measurement of reflected and emitted radiation from the Earth's surface is subject to problems such as variable illumination and atmospheric conditions. In addition, the sensor itself is subject to variations in performance. As more quantitative global studies are being undertaken, a number of data problems have been identified (Justice *et al.*, 1989; Goward *et al.*, 1993; Gutman and Ignatov, 1995) with the most serious problems found in the GVI time series, as noted by Kineman and Ohrenschall (1992), being orbital drift and radiometric discontinuities at satellite changeovers. Orbital drift results in changes of sun-sensor-target geometry due to a slowing of the satellites in orbit. An important consequence of this problem is an increasing NDVI through time over low vegetation areas, especially desert regions. As the satellite passes later and later in the afternoon the pathlength of solar radiation increases and the shorter wavelength red light attenuates faster than the longer NIR light, thus making NDVI values rise, creating a false interpretation of increasing vegetation. Radiometric discontinuities are a result of detector and/or elevation degradation over the life of the sensor that results in discontinuities between the calibration of successive satellites (Los *et al.*, 1994). The AVHRR sensors have no internal visible and NIR calibration and so various pre- and post-launch calibrations have been used with varying degrees of success (Roderick *et al.*, 1996).

[1]NDVI is derived by dividing the difference between the NIR and red images by the sum of the NIR and red images (Channel 2 − Channel 1)/(Channel 2 + Channel 1) (Kidwell, 1994).

Clark Labs for Cartographic Technology and Geographic Analysis, George Perkins Marsh Institute, Clark University, Worcester, MA 01610.

S.S. Young is presently with the Geography Department, Salem State College, 352 Lafayette Street, Salem, MA 01970-5353 (syoung@dgl.salem.mass.edu).

Photogrammetric Engineering & Remote Sensing, Vol. 65, No. 6, June 1999, pp. 679–688.

0099-1112/99/6506–679$3.00/0

To overcome known problems in the GVI data, a new data set, the NOAA/National Aeronautics and Space Administration (NASA) Pathfinder AVHRR Land (PAL) data set has been reprocessed from the original GAC data using new algorithms in an attempt to eliminate known problems in the GVI data (Agbu and James, 1994). Gutman and Ignatov (1995) analyzed the application of post-launch calibrations used in the PAL data set (Rao and Chen, 1994) and found that the calibration removed both the effect due to orbital drift in the NOAA-9 data, and the discontinuity upon launch of NOAA-11. However, a small residual trend of increasing NDVI over the Sahara was still detected for most of the NOAA-11 period. Prince and Goward (1996) and Smith *et al.* (1997) have found that the new calibrations in the PAL data have improved the visible and NIR measurements, especially with respect to the calibration discontinuity effect between the three successive sensors on NOAA-7, -9, and -11. Young (1997), however, has found that, although partially diminished, the sensor-related problem of calibration discontinuity persists in the PAL data along with a spatial misregistration problem. These two problems in the PAL data will be investigated in this paper.

This research, spanning the years 1982 to 1992, uses the land covers of China to determine if the PAL data set has fully removed the major calibration problems which have plagued the earlier GVI data sets. The research uses the IDRISI Geographic Analysis System and the IDRISI Times Series Analysis (TSA) procedure (Eastman, 1995), based on standardized Principal Components Analysis, to analyze the data. The authors have found this form of analysis to be an effective way to identify problems in GAC-derived time series data.

Data

To date, there have been only a few comprehensive global-scale remote sensing land-cover data sets established. This research uses two of them, NOAA's Weekly Maximum Value Global Vegetation Index (GVI), extracted from the United Nations Environment Programme Global Resources Information Database (UNEP-GRID) at a 16-km spatial resolution (UNEP-GRID, 1992; Kidwell, 1995), and NOAA/NASA's Pathfinder AVHRR Land (PAL) data set with an 8-km resolution (Agbu and James, 1994). The data are derived from the AVHRR sensor on-board NOAA's Polar Orbiting Environmental Satellite series, specifically in this case, NOAA-7, -9, and -11.

The GVI data (April 1982 through December 1992) and the PAL data (January 1982 through December 1992) were in monthly maximum value composites (Holben, 1986), where the maximum NDVI value per pixel over the course of each month was used for that month (Agbu and James, 1994; Kidwell, 1994). The authors extracted the China data from the GVI and PAL data sets using the *China County Border File* (Lam, 1989). The PAL images originally were in the Goode's Interrupted Homolosine Projection, and were reprojected by the authors to a latitude/longitude projection[2]. At the end of the research, analyses were also run with the PAL data in the original projection, producing the same conclusions, which indicates that the reprojection algorithm did not introduce problem-causing artifacts in the data. The data needed to be reprojected so that various land-cover validation material could be used with the PAL data. The NDVI values (−1 to +1) for both data sets have been scaled 0 to 255.

For both the GVI and PAL data, annual average composites (1982 through 1992) were created for each year where 12 monthly images (January through December) were added together and then divided by 12, yielding an annual average NDVI image. These annual average NDVI composites were created to remove seasonal variation in the data in order to focus on inter-annual variation where the potential sensor-related problems of spatial misregistration, drift, and discontinuities would become evident. In the case of GVI, the data for 1982 began in April and, as a result, January, February, and March of 1983 were substituted in the creation of the annual average for 1982.

In the process of analyzing temporal changes in the GVI and PAL data, it was critical to determine the land-cover type where apparent changes were occurring. For identification of land covers where change was occurring, a number of digital and non-digital vegetation maps and images were used. The China information includes two global-scale digital land-cover maps, Olson's *World Ecosystems*, and Leeman's *Holdridge Life Zone Classifications* (Kineman and Ohrenschall, 1992); two non-digital paper vegetation cover maps, *The Vegetation of China* (Wu, 1980) and *Vegetation Map of China* (Hou 1983); two non-digital atlases, *Atlas of Forestry in China* (Xu, 1991) and *The National Economic Atlas of China* (Institute of Geography *et al.*, 1994); two paper Landsat images, one Landsat TM composite of all of China and one Landsat TM composite of the Great Black Dragon Fire in northern Heilongjiang in 1987; and six digital 1993 AVHRR LAC images (Heilongjiang, Ningxia, Fujian, Yunnan, Guizhou, and Sichuan). The "Percent Forest Cover Map" from *The National Economic Atlas of China* (Institute of Geography *et al.*, 1994) was digitized and used in the research to define forest cover areas (<10 percent, 10 to 19 percent, 20 to 29 percent, 30 to 39 percent, 40 to 49 percent, 50 to 60 percent, and >60 percent). The data for this map are from the late 1980s.

Methodology

Principal Components Analysis (PCA) was used to analyze the data sets. PCA is a multivariate statistical method which undertakes a linear transformation of a set of image bands to create a new set which is uncorrelated and ordered according to the amount of variance explained (from most to least) (Johnston, 1980). PCA can use *unstandardized components*, where bands with higher variability contribute more to the new component images, or standardized components, where every original band has equal weight in the creation of the new component bands (Singh and Harrison, 1985). PCA has most commonly been used with unstandardized components as a compression tool for remote sensing data where minor components with little explanatory information have been discarded. Some of the early studies utilizing the GVI database used the PCA methodology with unstandardized components to perform land-cover mapping (Tucker *et al.*, 1985; Townshend *et al.*, 1987). Fung and LeDrew (1987), along with Eastman (1992) and Eastman and Fulk (1993), have shown that standardized PCA appears to produce more useful components than unstandardized PCA for the analysis of land-cover change in multi-temporal image data sets. Eastman (1992) along with Eastman and Fulk (1993) explored the potential of using standardized PCA with GVI data for Africa to detect change in vegetation over time. Their research showed the potential usefulness of indicating various changes in vegetation such as seasonal changes between winter and summer or aseasonal changes such as the effects of El Niño/Southern Oscillation (ENSO) events. Their research also showed the ability of the PCA methodology to identify sensor-related problems with time series GVI data. Further studies (Anyamba, 1994; Anyamba and Eastman, 1996) have shown the ability of the PCA methodology with AVHRR-derived NDVI data to detect climatically driven vegetation variation over long periods of time as well as to identify sensor

[2]Projection program supplied by B. B. Ding of NASA Goddard.

related changes in the data. These studies, and most other landcover change GVI and PAL studies, use the data in monthly or dekadal composites while this study uses the data in annual composites.

The standardized PCA employed in this study uses a time series of AVHRR data with the same area (China) and the same spectral wavelength (NDVI) for each scene. The only variation in the data is time, and, therefore, the procedure could be considered a "chronological standardized PCA." The procedure creates two products: component images (spatial output) and component loadings (temporal output). The first component image presents the spatial pattern which best describes the greatest degree of variability among the input images. The first component's loadings describe the degree to which each of the original images is correlated to the component and thus produces a time signal of variability. With time series AVHRR NDVI data, as is the case in this study, generally all of the input images are highly correlated (nearly 100 percent) with Component 1. Land covers from year to year do not change dramatically compared to how they change spatially. That is, the difference in scaled NDVI between a desert (120s) and a tropical evergreen forest (210s) is greater than the annual changes between the same pixels in the desert (i.e., 1984: 122; 1986: 122.6) and the same pixels in the forest (1984: 211; 1986: 210). Therefore, Component 1 of a standardized PCA of annually composited data always has a very high percent of variance, and the component's image represents the characteristic value over the whole series.

Because each of the successive components (2, 3, 4, etc.) is uncorrelated with Component 1 and each other, they represent statistically orthogonal (independent) factors which are isolated from other factors. These orthogonal factors represent variation (during the time period) from the overall general characteristic as displayed in Component 1 (Eastman, 1992; Eastman, 1995). Each successive component decreases in magnitude, that is, the early components represent variation with either (or both) extensive spatial characteristics or intense temporal characteristics. Although each component after Component 1 can be the combination of a variety of changes occurring in the data, each tends to be dominated by one activity and its related effects, especially for early components (Eastman and Fulk, 1993). Even though the components following Component 1 have a low percent of variance, and low eigenvalues, they are significant in that they represent variation which has occurred in the data relative to its "average" condition (Component 1). The chronological standardized PCA procedure is sensitive to subtle changes in the data. The process can be considered similar to the study of successive residuals. The objective of the chronological standardized PCA methodology, using the same geographic area and the same spectral wavelength over time, is to isolate and analyze these variations while the unstandardized PCA methodology, using different spectral bands of data over the same area, is to remove redundancy from remote sensing bands and discard components with low values. An important point is that, with a standardized PCA using NDVI data, the loadings also represent how NDVI varies in the component over time.

Results and Discussion

Overview

The research began by using the chronological standardized PCA procedure with the annual average GVI data for China to evaluate the known sensor problems in the data. This analysis demonstrated problems of radiometric miscalibration between satellites and orbital drift. The problem of large radiometric shifts at the point of satellite change was clearly evident in the loadings for Component 2 (Figure 1c) which show large shifts between 1984–1985 and 1988–1989. These radiometric shifts in the GVI data are well documented elsewhere (Kineman and Ohrenschall, 1992; Eastman and Fulk, 1993). The problem of orbital drift, which is related to the issue of radiometric shifts, was also evident in Component 2. The loadings (Figure 1c) show a continuous decrease in NDVI throughout each satellite period[3]. Temporal profiles of the Taklimakan desert, using the original GVI annual average images, also clearly show orbital drift with increasing NDVI for this sparsely vegetated region, especially for NOAA-9 (Figure 2). There is no documented evidence of this desert region increasing in NDVI throughout the 1980s, and there is evidence that other arid regions in the world experienced a similar increase in NDVI due to orbital drift (Kaufman and Holben, 1993).

Next, a chronological standardized PCA for China was executed with the annual average PAL data. The resulting first four components created virtually the same configurations (images and loadings) as in the GVI data, though in a different sequence (Figure 1) (Young, 1997). This means that either the PAL data still have the sensor-related problems, or that the changes which occurred to China's vegetation coincided with the known sensor problems in the GVI data. In PAL components two through four, we chose pixels which were most highly (top 25 percent) related to the loadings (positively and negatively) and investigated for a number of plausible causes of land-cover change, including natural hazards and climate change as well as human-induced change such as urbanization, pollution, agricultural development, deforestation, and reforestation. Concerning Components 2 and 3, we could not find any published patterns which matched the loadings and spatial locations of potential changes due to natural effects (Ding, 1994; Fu, 1995; Shi, 1995) or human activity (Richardson, 1990; He, 1991; Smil, 1993; Luo, 1995; Wang, 1995). It was concluded that changes depicted in these components were most likely due to similar exogenous factors which influenced the GVI data. The spatial patterns and temporal loadings for Component 4, however, do show changes associated with human activity (agricultural intensification and deforestation), and later components show various climatic effects in addition to human activity on China's land cover. The scope of this paper does not allow for the discussion of these later components (forthcoming article). Investigations of the PAL data for China led to the conclusion that for the period of 1982 to 1992 the problem of orbital drift was successfully minimized for arid regions, but the problem of radiometric miscalibration at satellite changeovers persists in the PAL data. In addition, it was discovered that both the PAL data and GVI data suffer from a spatial misregistration, especially the data from NOAA-9 relative to the data from NOAA-7 and -11. This spatial misregistration was not discovered until the PAL data were analyzed extensively.

Orbital Drift in PAL Data

The chronological standardized PCA of the PAL data shows potential orbital drift in Component 3 with decreasing NDVI in loadings for NOAA-11, especially for 1990 through 1992 (Figure 1c). Arid and semi-arid regions are negatively associated with these loadings, and thus slightly increasing in NDVI (Figure 1c, Plate 1). The pattern is similar to GVI Component 2 which showed orbital drift (Figure 1c). The orbital drift, however, seems to be greatly reduced in the PAL data relative to the GVI data (Figure 1c). Perhaps more importantly, profil-

[3]1985 has a slightly lower NDVI than 1986 because the data for the first three months of 1985 are from NOAA-7 and thus 1985's yearly average was influenced by NOAA-7's lower values.

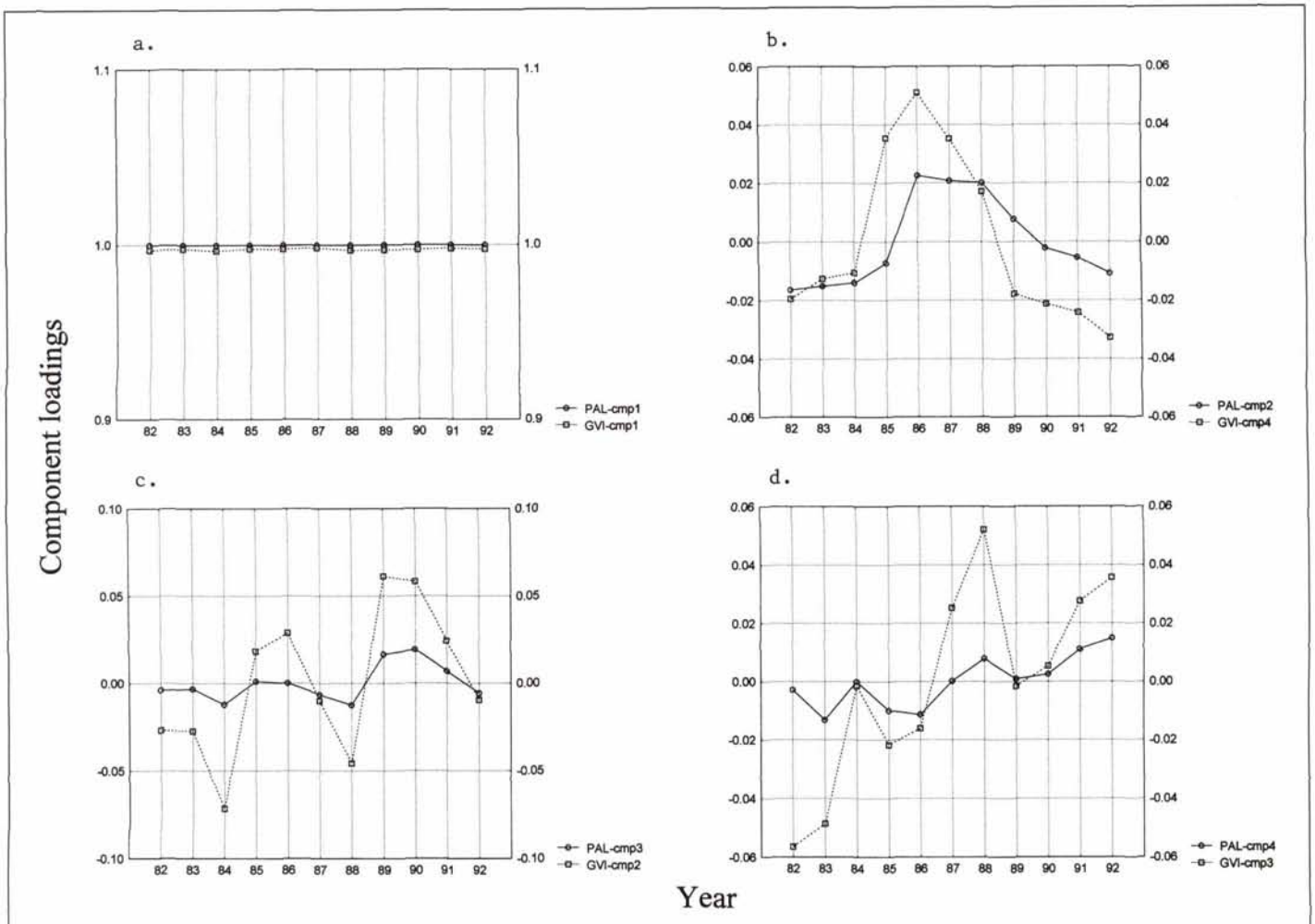

Figure 1. Component loadings of PAL and GVI data. (a) GVI and PAL Component 1. (b) PAL Component 2, GVI Component 4. (c) PAL Component 3, GVI Component 2. (d) PAL Component 4, GVI Component 3.

ing the original annual average PAL data for arid regions, such as the Taklimakan desert (Figure 2), the PAL data show that the effects of orbital drift have been minimized except for a slight drift for NOAA-11 which has also been noted by Gutman and Ignatov (1995).

Radiometric Miscalibration for PAL Data

Analysis of PAL Component 3 shows a potential radiometric miscalibration of the PAL data. The loadings for Component 3 show distinctive breaks at the satellite changeover periods (Figure 1c). This component is similar to Component 2 of the GVI data which showed the radiometric miscalibration. The loadings for this component, however, seem to show that the radiometric miscalibration between satellites has been reduced, especially for NOAA-7/NOAA-9, though not completely. Although Component 3 could be showing a number of changes taking place, there are no documented large-scale land-cover changes occurring in China with such distinctive characteristics, as indicated by the loadings, in the regions, as indicated by the image (Figure 1c, Plate 1). The component loadings also show that over the course of the 11 years (1982 through 1992), NDVI slightly increases. The component image shows forest regions in southeastern and northeastern China positively correlated, thus increasing in NDVI, with north and west China primarily negatively correlated, and thus decreasing in NDVI. Looking at the trends of individual satellites (1982 through 1984, 1985 through 1988, 1989 through 1992), however, each trend is decreasing, not increasing, and thus the areas increasing in NDVI according to

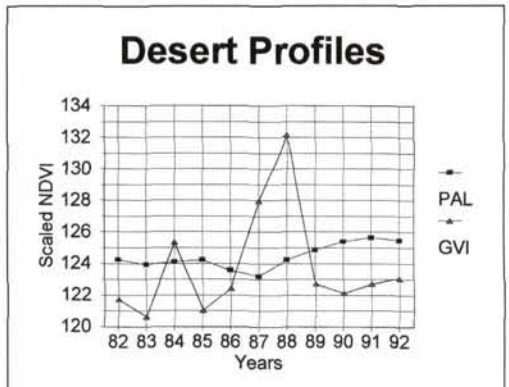

Figure 2. Temporal profiling of the Taklimakan Desert of western China for the PAL and GVI data. Each annual value is an average of Taklimakan Desert pixels for that year for that data set. The location of the Taklimakan Desert in each data set is based on Hou (1983).

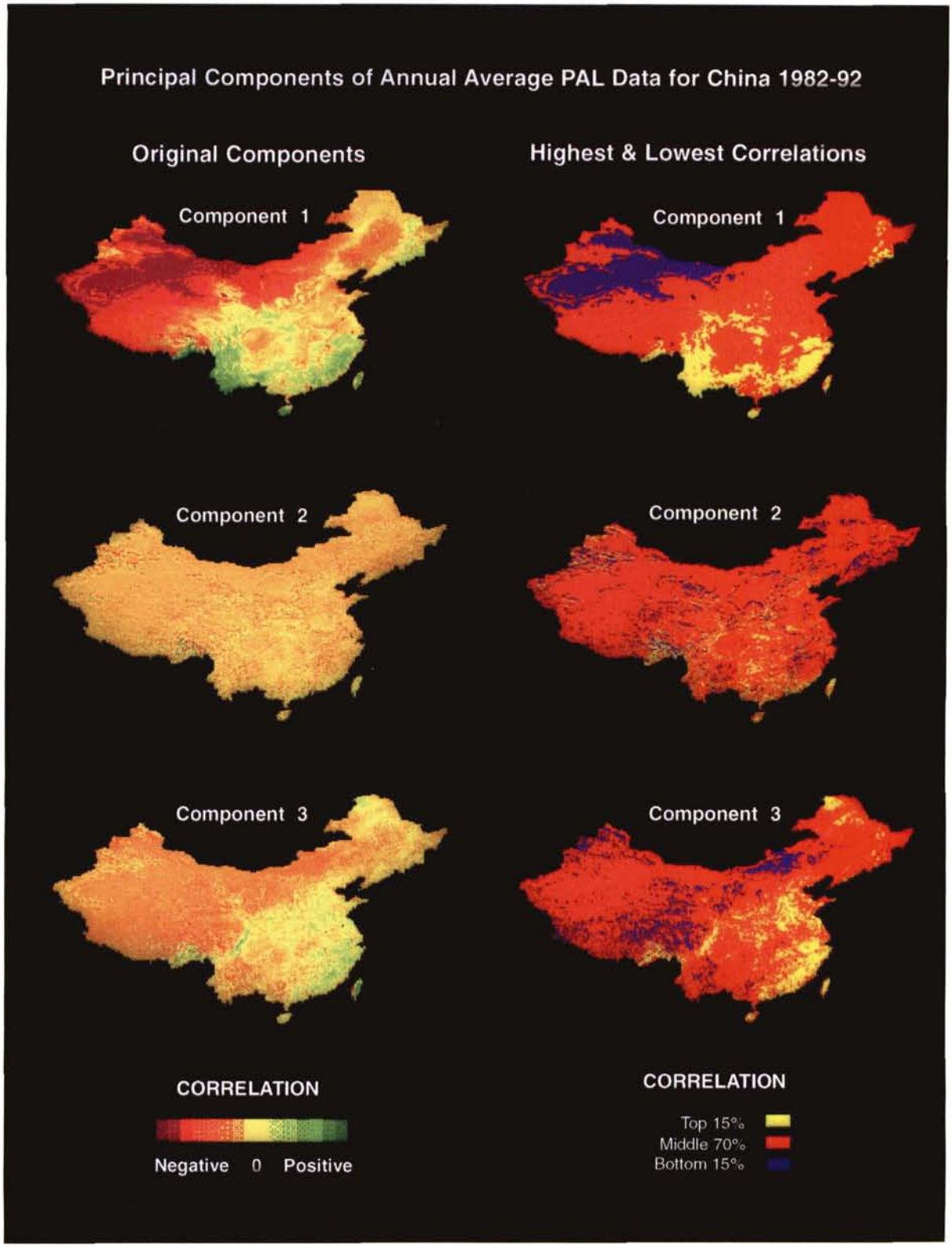

Plate 1. Color images of the PAL data standardized Principal Components Analysis (1982–92) Components 1, 2, and 3. The left-hand column of images are the original components linearly stretched with values ranging from 0 to 255. The right-hand column of images are value-sliced images of top 15 percent, middle 70 percent, and bottom 15 percent of component image values. That is, the pixels with a yellow color are the top 15 percent of pixels most correlated with the loadings for their particular component, and the blue colored pixels are the 15 percent of pixels most negatively correlated with loadings, or those with the opposite trend of the loadings.

TABLE 1. TOP AND BOTTOM 25 PERCENT OF PAL COMPONENT3[1] CROSS-TABULATION WITH TOP AND BOTTOM 25 PERCENT OF PAL SINGLE SATELLITE COMPOSITE[2]

		PAL Single Satellite Composite	
		Bottom 25%	Top 25%
C M P 3	Bottom 25%	406 pixels	10,485 pixels
	Top 25%	10,433 pixels	470 pixels

[1]PAL Component 3 from a chronological standardized PCA of annual images 1982 through 1992.

[2]A single composite image of increasing NDVI from 1982 to 1992 was made from three components from a chronological standardized PCA run for each of the NOAA satellites (NOAA−7, −9, −11). The three components indicating increasing NDVI were added together with the resulting image divided by 3, creating a composite image which minimizes radiometric miscalibration between satellites.

the whole series, might actually be decreasing according to the individual satellite periods (Figure 1c). Therefore, the overall increase in NDVI for the entire 11 years seems to be the result of a radiometric miscalibration at the point of satellite changeover. To investigate this further, a chronological standardized PCA was run for each of the individual satellites (NOAA-7, -9, and -11), and each produced a component with decreasing NDVI in the loadings virtually the same as for the individual satellite years in the loadings of Component 3 above (Young, 1997). Adding these three components (weighted averages) from NOAA-7, -9, and -11 together and then dividing the resulting image by three creates an image depicting change over the entire 11-year period, minimizing the inter-satellite calibration problem. The resulting image is virtually a reverse image of Component 3 with forest areas associated with decreasing NDVI. A cross-tabulation between

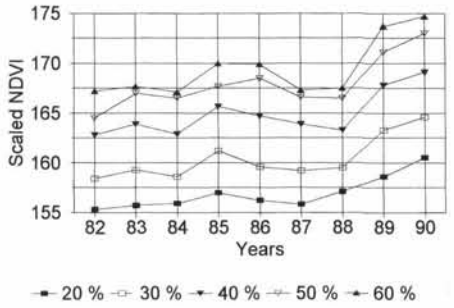

Figure 3. Annual profiles of percent forest cover from 1982 to 1990. Pixels used in profiles were determined by the "Percent Forest Cover Map" from *The National Economic Atlas of China* (Institute of Geography *et al.*, 1994), which was digitized by the authors, and uses the same categories as in the paper map (<10%, 10–19%, 20–29%, 30–39%, 40–49%, 50–60%, >60%). The data for this map are from the late 1980s. Note an increasing upward shift in values between 1988 and 1989 for areas with an increasing percent of forest cover.

Component 3 and the single-satellite composite image shows that almost pixel for pixel the two images are completely opposite from each other with complete opposite interpretations (Table 1). This indicates that there must be some form of radiometric miscalibration between the satellites in order to produce this opposite effect. Forests in particular seem to be differentially influenced by the shift in satellites because forest areas are highly correlated with Component 3 while other land covers are not. Looking at the annual profiles of percent forest cover (as defined by The Institute of Geography *et al.* (1994)), with an increasing percent of forest cover there seems to be clearer evidence of the satellite changeover, especially between NOAA-9 and -11 (Figure 3). Profiles of arid regions, however, show very little miscalibration in the PAL data while there is a clear miscalibration in the GVI data (Figure 2). A differential radiometric miscalibration may have been created in the PAL data because desert areas were used to create algorithms for PAL data recalibration. The authors suspect that the reason why forests may still show a radiometric miscalibration is that they react differently than do deserts to electromagnetic radiation because deserts reflect highly in red and NIR while forests absorb highly in red and reflect highly in NIR. Atmospheric conditions are also different over forests than over desert regions. Therefore, it is possible that the algorithm written for desert reflectance might not completely remove the problem of sensor degradation for all land-cover types. However, it is noted that the scale of radiometric miscalibration found in forests has been reduced in the PAL data relative to the GVI data, though not removed as in arid land covers. Further investigation in this area needs to be undertaken.

Spatial Misregistration for PAL Data

Spacial misregistration, although noted in the literature (Goward *et al.*, 1993), is not often considered a major problem with the GVI and PAL data. However, this study shows that it might be an important problem when analyzing land-cover change over time. Component 2 of the PAL data produced an unusual image and loadings. The loadings for Component 2 are an upside down "U" shape with low values in the early 1980s and 1990s but with high values in the mid 1980s (Figure 1b). The image for Component 2 shows that both positively and negatively correlated areas are quite widespread in China without clear segregation as found in the first component and all of the other components (Plate 1). Not only are they widely distributed, but many of the positive and negative pixels are seen next to each other, especially in mountainous areas. An initial evaluation suggested that this component was showing signs of the 1986/87 ENSO event, or another climatic event which caused a major shift in wind patterns and associated precipitation, thus changing growth characteristics on different sides of the mountains. Analysis into the climate of China during the 1980s did not reveal this kind of weather pattern (Ding, 1994). GVI Component 4 showed a similar pattern (Figure 1b) and indicates a potential misregistration of the data. The GVI loadings have a clear break at the points of satellite change (1984–1985, 1988–1989), and the loadings for NOAA-7 and NOAA-11 are similar throughout their tenure, with the variation primarily coming from the loadings for NOAA-9, indicating that there might be some form of misregistration for NOAA-9 relative to NOAA-7 and NOAA-11. The breaks in PAL Component 2 (1985–1986, 1987–1988–1989) are not as clearly associated with the satellite switches, and thus it is possible that a calibration formula used in the PAL data smoothed the misregistration problem instead of removing it; thus, the data from NOAA-7 and -11 are skewed by the NOAA-9 data.

Further analysis into the component image found that not only were mountainous areas exhibiting this effect, but

TABLE 2. ANALYSIS OF MISREGISTRATION THROUGH PAL PIXEL VALUES IN LAKE KHANKA[1]

NOAA-7				NOAA-9				NOAA-11			
1982				1985				1989			
166	164	153	156	166	162	156	158	164	166	159	156
156	155	152	156	159	156	156	160	164	163	158	158
126	***120***	***121***	***123***	***134***	***124***	***132***	144	150	140	***134***	***138***
1983				1986				1990			
162	162	154	156	162	164	157	157	167	166	160	156
153	154	156	154	167	163	154	156	162	161	156	156
125	***122***	***122***	***123***	154	153	153	154	148	***134***	***134***	***129***
1984				1987				1991			
161	159	152	151	158	161	156	156	166	166	161	157
154	153	150	151	163	160	154	157	161	160	158	157
138	***126***	***128***	***125***	153	152	151	153	149	145	***139***	***137***
				1988				1992			
				160	160	154	155	162	160	152	157
				164	161	152	155	153	153	152	152
				154	154	152	152	***135***	***129***	***125***	***124***

[1]Bold italic numbers are values below 140, representing general lake values for scaled NDVI. The numbers in the table are the raw pixel values of scaled NDVI for the Lake Khanka region. The bottom line of each year is in an unmasked portion of the lake.

so were lake shores, river valleys, and oases; thus, this change could not be explained by the hypothesis of wind/precipitation change. To investigate the possibility of spatial misregistration, four lake areas (Khanka, Hongze, Tai, and Poyang) were intensively analyzed. Visually inspecting the images and quantitatively reviewing the raw pixel values, it is evident that there is a shift in pixel values. The shift in values coincides closely with the patterns created in the loadings where values for NOAA-9 are clearly different from those of NOAA-7 and -11, especially for the GVI data. Scaled NDVI lake values tend to be in the 120s and low 130s while lake shore vegetation tend to be in the 140s or higher; thus, the shifting of values between the 120s and the 140s indicates the shifting of pixels due to a spatial misregistration.

TABLE 3. LAKE KHANKA PAL PIXEL VARIATION

	Pixel 1[1]		Pixel 2[2]		Pixel 3	
Year	Value[3]	Anomaly[4]	Value	Anomaly	Value	Anomaly
1982	123	−13.5	156	−3.5	156	3
1983	123	−13.5	153	−6.5	153	0
1984	125	−11.5	154	−5.5	154	1
1985	144	7.5	159	−0.5	159	6
1986	154	17.5	167	7.5	154	1
1987	153	16.5	163	3.5	153	0
1988	152	15.5	164	4.5	154	1
1989	138	1.5	164	4.5	150	−3
1990	129	−7.5	162	2.5	148	−5
1991	137	0.5	161	1.5	149	−4
1992	124	−12.5	153	−6.5	153	0
Average[5]:	136.5		159.5		153	
Anomaly[6]:		58.5		24		12

[1]Pixel 1 is a lake border pixel.
[2]Pixels 2 and 3 are the same pixel, an interior forest pixel, but pixel 3's values shift as the data shifts between satellites as best could be determined based on the loadings.
[3]These values are raw scaled NDVI values.
[4]The anomaly is the difference between the raw NDVI value for the year and the average NDVI value over the 11-year period (yearly value minus 11-year average).
[5]Average NDVI value for the pixel over the 11-year period.
[6]Accumulated variation from the 11-year mean, i.e., sum of the positive anomaly values which equal the sum of negative anomaly values ± 1.

Although most lake pixels have been masked out in the PAL data, there were some unmasked pixels found in China. Table 2 shows pixel values near Lake Khanka (Heilongjiang) for each of the PAL annual averages from 1982 to 1992. The table shows NOAA-7 lake value pixels (120s) shifting to vegetation values (140s) for NOAA-9 and back to lake values later in NOAA-11 in a fashion similar to the loadings. Three pixels near Lake Khanka (Table 3) were selected to investigate the potential influence of the misregistration on pixel anomaly values (annual average minus the 11-year average). Of the three pixels, pixel 1 was a lake-shore pixel (extreme case), pixel 2 was an interior forest pixel, a milder case, and pixel 3 was the same as pixel 2, except that the values were artificially shifted with the misregistration (creating a situation with a minimum of spatial misregistration). The shifting values for pixel 3 were estimated based on the loadings for Component 2. Pixel 1 had an anomaly range four times greater than pixel 3, and pixel 2 had more than a two-fold increase over pixel 3. The positive and negative anomalies for pixels 1 and 2 show the general changes between satellites while pixel 3 does not. A similar analysis of Lake Hongze in Jiangsu province also clearly shows this form of spatial misregistration. Figure 4 shows a shift in NDVI (primarily a southward movement of pixels) for 1986 through 1988 relative to 1982 through 1985 and 1989 through 1992, which the loadings of Component 2 show. This shift is particularly clear for the central portion of the image. This analysis indicates that Component 2 is potentially showing a spatial misregistration of the data at the pixel level. It also shows that changes in the spatial registration of pixels can create a large change in values, especially for pixels along the border between different land-cover types. This is why mountainous areas along with river valleys, oases, and lake shores were prominent in Component 2. The pixels in Component 2 are quite widespread throughout China and not congregated as in the other components, especially for the highest and lowest correlated pixels (Plate 1).

Conclusion

The known sensor problems found in the GVI data are also found in the PAL data, though they seem to be diminished as the percent of variation, and the eigenvalues for Components 2 through 4 in the PAL data have decreased relative to the GVI data (Figure 1, Table 4). The chronological standardized

TABLE 4. PERCENT VARIANCE AND LOADINGS FOR PAL AND GVI ANNUAL AVERAGE CHRONOLOGICAL STANDARDIZED PRINCIPAL COMPONENTS ANALYSIS

PAL data	CMP 1	CMP 2	CMP 3	CMP 4	CMP 5	CMP 6	CMP 7	CMP 8	CMP 9	CMP 10	CMP 11
% Variance	99.94175	0.02088	0.01010	0.00749	0.00355	0.00328	0.00290	0.00266	0.00264	0.00253	0.00224
Loadings:											
1982	0.99971	−0.01641	−0.00394	−0.00282	−0.00452	−0.00568	−0.00154	−7E-06	0.00154	−0.01293	0.00162
1983	0.99973	−0.01508	−0.00337	−0.01318	0.00460	−0.00019	−0.01080	−0.00125	0.00331	0.00592	−0.00013
1984	0.99971	−0.01395	−0.01215	−2.2E-05	0.00113	0.00909	0.00833	−0.00830	−4.1E-05	0.00092	0.00078
1985	0.99974	−0.0072	0.00116	−0.00996	−0.00730	−0.00255	0.00814	0.00928	−0.00066	0.00533	−0.00096
1986	0.99959	0.02257	6.1E-05	−0.01136	0.00526	−0.00143	0.00116	−0.00240	−0.00774	−0.00346	−0.00668
1987	0.99967	0.02078	−0.00663	0.00015	8.9E-05	−0.00130	−0.00111	0.00071	−0.00256	0.00128	0.01259
1988	0.99963	0.02006	−0.01245	0.00782	−0.00692	0.00319	−0.00372	0.00177	0.00733	0.00031	−0.00566
1989	0.99974	0.00769	0.01664	0.00084	0.00678	−0.00326	0.00527	−0.00221	0.01049	−0.00038	0.00085
1990	0.99975	−0.00219	0.01940	0.00250	−0.00372	0.01183	−0.00419	0.00230	−0.00347	−0.00229	0.00093
1991	0.99980	−0.00545	0.00700	0.01110	−0.00631	−0.00858	−0.00153	−0.00755	−0.00488	0.00530	−0.00168
1992	0.99972	−0.01082	−0.00573	0.01492	0.01091	−0.00110	0.00000	0.00767	−0.00332	0.00000	−0.00165

GVI data	CMP 1	CMP 2	CMP 3	CMP 4	CMP 5	CMP 6	CMP 7	CMP 8	CMP 9	CMP 10	CMP 11
% Variance	99.44471	0.16193	0.10639	0.07679	0.04362	0.03612	0.03441	0.02805	0.02460	0.02361	0.019792
Loadings:											
1982	0.99686	−0.02683	−0.05651	−0.01943	−0.01561	−0.01533	0.02869	0.01461	−0.01620	0.00377	0.01066
1983	0.99733	−0.02750	−0.04859	−0.01265	0.00138	−0.01369	−0.03082	0.00339	0.02124	−0.00323	−0.01941
1984	0.99633	−0.07152	−0.00145	−0.01059	−0.00050	0.03404	−0.00706	−0.02757	−0.00538	0.00250	0.00983
1985	0.99758	0.01841	−0.02181	0.03533	0.03527	0.03060	0.00839	0.02090	−0.00491	−0.00396	−0.00830
1986	0.99738	0.02892	−0.01606	0.05091	−0.00775	−0.01476	0.01025	−0.02478	0.01440	−0.01579	0.01203
1987	0.99805	−0.01025	0.02527	0.03521	−0.00998	−0.01174	7.8E-05	−0.00250	−0.00592	0.03816	−0.01240
1988	0.99666	−0.04569	0.05203	0.01712	−0.01181	−0.01085	−0.01470	0.02304	−0.00945	−0.02218	0.00585
1989	0.99701	0.06130	−0.00158	−0.01781	0.00706	0.00045	−0.02874	0.00709	−0.00136	0.01344	0.02742
1990	0.99715	0.05839	0.00537	−0.02128	−0.01352	0.00205	−0.00422	−0.01582	−0.02742	−0.01305	−0.02051
1991	0.99775	0.02435	0.02766	−0.02415	−0.02873	0.02173	0.01975	0.01109	0.02849	0.00116	−0.00391
1992	0.99731	−0.00967	0.03565	−0.03271	0.04416	−0.02249	0.01836	−0.00946	0.00649	−0.00085	−0.00122

PCA of the annually composited PAL data suggests that the problems of spatial misregistration and radiometric miscalibration are still problems in the data set in that they are the second and third components and therefore are two significant variations observed in China's vegetation between 1982 and 1992 when analyzed at the annual level. As noted above in the Methodology section, an important aspect of the PCA procedure is that it arranges its components in a sequential fashion from most significant variation to least.

Each of the problems in the PAL data have differing influences on the interpretation of long-term change analysis. The effect of spatial misregistration on the interpretation of vegetation classification and vegetation change will vary depending on the scale of the analysis and the homogeneity of the land cover being analyzed. In general, the larger the area being studied, the less the influence of the spatial misregistration because other effects will become more influential. Spatial misregistration can potentially have a strong effect if one is working at the local scale. Perhaps more influential is the type of land cover in the area being analyzed. The more homogeneous the land cover, the less weight the spatial misregistration will have because there will be fewer variations between pixel values; therefore, other effects, such as climate change, will be more dramatic. Areas of greater heterogeneity, especially with radically different vegetation types with large differences in NDVI values, will be more influenced by spatial misregistration. Problems will arise because in these landscapes many pixels will experience large changes in values when spatial misregistration occurs. A large variety of land covers stretch over much of China to create a landscape of heterogeneity. The result is that China is dominated by many pixels of changing values, except for the large western arid region. This great heterogeneity found in China may be the reason why the problem of spatial misregistration appeared as having such a strong effect in China and may not be as important in more homogeneous areas. In the literature the spatial misregistration of the GAC data is linked to problems of navigation and are seen as being relatively inconsistent and random (Goward *et al.*, 1993). This study, however, shows an aspect of the spatial misregistration problem which seems to be related to the mapping of NOAA-9 data relative to NOAA-7 and -11.

The radiometric shift in values between satellites is a known problem in the GVI data. Early evaluations of the PAL data have suggested that the radiometric miscalibration between satellites was corrected because there are no longer any large shifts over the arid regions. This study, however, suggests that the calibration problem has not been fully fixed because shifts still exist over other land covers, especially forest covers. Concerning the interpretation of the PAL data, this radiometric miscalibration is a difficult problem because the effects of the radiometric miscalibration seem to vary depending on the land-cover type in question with a disproportionate effect on forest areas. Desert regions have been used to recalibrate the data to remove sensor related problems. Because different cover types react differently to red and NIR light, the study suggests that the recalibration has been successful for arid regions, but perhaps not as well for other cover types. Also important is the fact that initial evaluations of the PAL data have found certain regions correctly classified; therefore, current users are assuming that the radiometric problem has been completely corrected, even though it potentially has not been. Preliminary research in Africa also indicates that the radiometric problems are found in forested areas. The problem of orbital drift, however, was found to be successfully minimized in China for arid regions as has been found in Africa.

Despite these problems, the PAL data are still able to pull out significant changes which are truly occurring in land covers in China and Africa. The scope of this paper does not allow a review of the changes which were found to be occurring using the PAL data for China and Africa (forthcoming article).

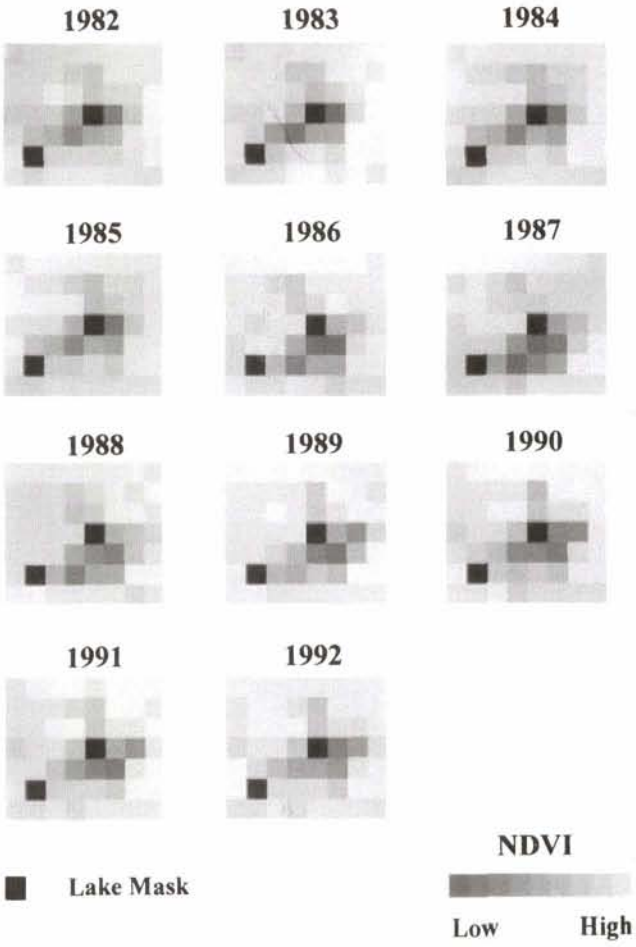

Figure 4. A 56-pixel window of the Hongze Lake region in Jiangsu Province for annual average PAL data for 1982 through 1992. The two prominent black squares are lake masks while the grey pixels are scaled NDVI ranging from 120 (darkest grey) to 191 (lightest grey). The low NDVI pixels near the center of the window appear to shift downward in 1986 to a new position for 1986, 1987, and 1988 with an upward transition in 1989, and returning to a position in 1990, 1991, and 1992 which is very similar to that in 1982, 1983, 1984, and 1985. These shifts in pixel values follow the pattern in the loadings for PAL Component 2.

Acknowledgments

The authors thank UNEP-GRID Geneva, especially Ron Witt, and NASA Goddard Space Flight Center, especially Peter Smith and B.B. Ding, in the acquisition of GVI and PAL data; Dr. J. Ronald Eastman of the Graduate School of Geography at Clark University for assistance and guidance on the manuscript; and the Art Department at Salem State College, especially Dave Borge, for assistance in the production of images. The authors also thank the anonymous reviewers for their thoughtful and helpful comments.

References

Agbu, P.A., and M.E. James, 1994. *The NOAA/NASA Pathfinder AVHRR Land Data Set User's Manual*, Goddard Distributed Active Archive Center Publication, Greenbelt, Maryland.

Anyamba, A., 1994. Retrieval of ENSO signal from vegetation index data, *The Earth Observer*, 6(3):24–26.

Anyamba, A., and J.R. Eastman, 1996. Interannual variability of NDVI over Africa and its relation to El Nino/Southern Oscillation, *International Journal of Remote Sensing*, 17:2533–2548.

Box, E.O., B. Holben, and V. Kalb, 1989. Accuracy of the AVHRR vegetation index as a predictor of biomass, primary productivity and net CO_2 flux, *Vegetatio*, 80:71–89.

DeFries, R., M. Hansen, and J. Townshend, 1995. Global discrimination of land cover types from metrics derived from AVHRR Pathfinder data, *Remote Sensing of Environment*, 54:209–222.

Ding, Y.H., 1994. *Monsoons over China*, Kluwer Academic Publishers, Boston.

Eastman, J.R., 1992. Time series map analysis using standardized principal components, *ASPRS/ACSM/RT 92 Technical Papers, Global Change and Education*, 3–8 August, Washington, D.C., 1:195–204.

———, 1995. *Idrisi for Windows. Version 1.0*, Clark Labs for Cartographic Technology and Geographic Analysis, Clark University, Worcester, Massachusetts.

Eastman, J.R., and M. Fulk, 1993. Long time series evaluation using standardized principal components, *Photogrammetric Engineering & Remote Sensing*, 59(6):991–996.

Ehrlich, D., J.E. Estes, and A. Singh, 1994. Review article: Applications of NOAA-AVHRR 1 km data for environmental monitoring, *International Journal of Remote Sensing*, 15:145–161.

Fu, C.B., 1995. Regional effects of global warming in China, *Elements of Change 1995* (S.J. Hassol and J. Katzenberger, editors), Aspen Global Change Institute, Aspen, Colorado, pp. 211–213.

Fung, T., and E. LeDrew, 1987. Application of principal components analysis to change detection, *Photogrammetric Engineering & Remote Sensing*, 53:1649–1658.

Goward, S.N., D.G. Dye, S. Turner, and J. Yang, 1993. Objective assessment of the NOAA global vegetation index data product, *International Journal of Remote Sensing*, 14:3365–3394.

Gutman, G., and A. Ignatov, 1995. Global land monitoring from AVHRR: potential and limitations, *International Journal of Remote Sensing*, 16:2301–2309.

He, B.C., 1991. *China on the Edge: The Crisis of Ecology and Development*, China Books & Periodicals, San Francisco.

Holben, B.N., 1986. Characteristics of maximum-value composite images of temporal AVHRR data, *International Journal of Remote Sensing*, 7:1417–1434.

Hou, H.Y., 1983. Vegetation of China with reference to its geographical distribution, *Annals of the Missouri Botanical Gardens*, 70: 509–548.

IGBP (The International Geosphere-Biosphere Programme), 1994. *IGBP in Action: 1994–1998*, IGBP Report # 28, Stockholm.

Institute of Geography, Chinese Academy of Sciences; National Economic Information Centre; and the Statistical Institute of the State Statistical Bureau, 1994. *The National Economic Atlas of China*, Oxford University Press, Hong Kong.

Johnston, R.J., 1980. *Multivariate Statistical Analysis in Geography*, Longman, New York.

Justice, C.O., B.L. Markham, J.R.G. Townshend, and R.L. Kennard, 1989. Spatial degradation of satellite data, *International Journal of Remote Sensing*, 10:1539–1561.

Kaufman, Y.J., and B.N. Holben, 1993. Calibration of the AVHRR visible and near-ir bands by atmospheric scattering, ocean glint and desert reflection, *International Journal of Remote Sensing*, 14: 21–52.

Kidwell, K.B. (editor), 1994. *Global Vegetation Index Users Guide*, National Oceanic and Atmospheric Administration, Washington, D.C.

———, 1995. *NOAA Polar Orbiter Data Users Guide (TIROS-N, NOAA-6, -7, -8, -9, -10, -11, -12, -13, and -14)*, National Oceanic and Atmospheric Administration, Washington, D.C.

Kineman, J.J., and M.A. Ohrenschall, 1992. *Global Ecosystem Database Version 1.0: Disc A, Documentation Manual*, Key to Geophysical Records Documentation No. 27, USDOC/NOAA National Geophysical Data Center, Boulder, Colorado.

Lam, N., 1989. *The China County Border File*, Arc/Info vector map of China's provinces, municipalities, and counties, Department

of Geography and Anthropology, Louisiana State University, Baton Rouge, Louisiana.

Los, S.O., C.O. Justice, and C.J. Tucker, 1994. A global 1° by 1° NDVI data set for climate studies derived from the GIMMS continental NDVI data, *International Journal of Remote Sensing*, 15:3493–3518.

Luo, C., 1995. Acid deposition and ozone monitoring and modeling in China, *Elements of Change 1995* (S.J. Hassol and J. Katzenberger, editors), Aspen Global Change Institute, Aspen, Colorado, pp. 233–235.

Malingreau, J.P., G. Stevens, and C. Fellows, 1985. 1982–83 forest fires of Kalimantan and North Borneo: Satellite observations for detecting and monitoring, *AMBIO*, 14:314–346.

NAS (National Academy of Sciences), 1990. *Research Strategies for the U.S. Global Change Research Programme*, National Academy of Sciences National Research Council Report, National Academy Press, Washington, D.C.

Prince, S.D., and S.N. Goward, 1996. Evaluation of the NOAA/NASA Pathfinder AVHRR Land Data Set for global primary production modelling, *International Journal of Remote Sensing*, 17:217–221.

Rao, C.N.R., and J. Chen, 1994. *Post-Launch Calibration of the Visible and Near-Infrared Channels of the AVHRR on NOAA-7, -9, and -11 Spacecraft*, NOAA Technical Report NESDIS 78, USDoC, Washington, D.C.

Richardson, S.D., 1990. *Forests and Forestry in China*, Island Press, Washington, D.C.

Roderick, M., R. Smith, and G. Lodwick, 1996. Calibrating long-term AVHRR-derived NDVI imagery, *Remote Sensing of Environment*, 58:1–12.

Shi, P.J., 1995. Natural hazards and disasters in China, *Elements of Change 1995*, (S.J. Hassol and J. Katzenberger, editors), Aspen Global Change Institute, Aspen, Colorado, pp. 244–247.

Singh, A., and A. Harrison, 1985. Standardized principal components, *International Journal of Remote Sensing*, 6:883–896.

Smil, V., 1993. *China's Environmental Crisis: An Inquiry into the Limits of National Development*, M.E. Sharpe, Armonk, N.Y.

Smith, P.M., S.N.V. Kalluri, S.D. Prince, and R. DeFries, 1997. The NOAA/NASA Pathfinder AVHRR 8-Km Land Data Set, *Photogrammetric Engineering & Remote Sensing*, 63(1):12–13, 27–32.

Tateishi, R., and K. Kajiwara, 1992. Global land cover monitoring by AVHRR NDVI data, *Earth Environment*, 7:4–14.

Thomas, I.L., R.W. Saunders, and D.L. Croom (editors), 1989. Applications of AVHRR data: Special issue, *International Journal of Remote Sensing*, 10:597–936.

Townshend, J.R.G. (editor), 1992. *Improved Global Data for Land Application: A Proposal for a New High Resolution Data Set*, International Geosphere-Biosphere Programme (IGBP) Global Change Report No. 20, IGBP, Stockholm.

Townshend, J.R.G., C.O. Justice, and V.T. Kalb, 1987. Characterization and classification of South American land covertypes using satellite data, *International Journal of Remote Sensing*, 8:1189–1207.

Tucker, C.J., J.A. Gatlin, and S.R. Schneider, 1984. Monitoring vegetation in the Nile Delta with NOAA-6 and NOAA-7 AVHRR imagery, *Photogrammetric Engineering & Remote Sensing*, 50:53–61.

Tucker, C.J., J.R.G. Townshend, and T.E. Goff, 1985. African land-cover classification using satellite data, *Science*, 227:369–375.

UNEP/GRID (United Nations Environment Programme/Global Resource Information Database), 1992. *UNEP/GRID Documentation Summary for Data Set*, UNEP/GRID, Geneva.

Wang, S.J., 1995. Industrialization and Urbanization in China, *Elements of Change 1995* (S.J. Hassol and J. Katzenberger, editors), Aspen Global Change Institute, Aspen, Colorado, pp. 259–261.

Wu, Z.Y., 1980. *The Vegetation of China*, Science Press, Beijing, (in Chinese).

Xu, Y.F., (editor), 1991. *Atlas of Forestry in China*, Bureau of Forestry, Beijing, (in Chinese).

Young, S.S., 1997. *The Use of Coarse-Grain, Global-Scale Remote Sensing Data to Analyze Forest Cover, Extent and Change, in China, 1982–1992*, dissertation, Clark University, Worcester, Massachusetts.

(Received 03 February 1997; revised and accepted 06 August 1998; revised 02 September 1998)